Nano-resolution in vivo 3D orbital tracking system to study cellular dynamics and bio-molecular processes

Ulas C. Coskun[1,*], Matthew L. Ferguson[2,3,*], Alexander Vallmitjana[4], Anh Hyunh[2], Julianna Goelzer[3], Yuansheng Sun[1], Shih-chu "Jeff" Liao[1], Sunil Shah[1], Enrico Gratton[4], and Beniamino Barbieri[1]

[1] ISS, Inc., 1602 Newton Drive, Champaign, IL 61822, USA.
[2] Department of Physics, Boise State University, Boise, ID, 83725, USA.
[3] Biomolecular Sciences Graduate Program, Boise State University, Boise, ID, 83725, USA.
[4] Laboratory for Fluorescence Dynamics, Department of Biomedical Engineering, University of California, Irvine, CA, 92697, USA.

[*] Author to whom correspondence should be addressed: Ulas C Coskun (ulas.coskun@iss.com) and Matthew L. Ferguson (mattferguson@boisestate.edu)

ABSTRACT

We present a microscopy technique, orbital particle tracking, in which the scanner scans orbits around species, unlike a raster imaging technique in which the scanner scans an area one line at a time. By analyzing the fluorescence emission intensity variation along an orbit, the location of a species in the orbit can be determined with precision of a tenth of a nanometer in a millisecond time scale, and the orbit can be moved to the new location of the species through a feedback loop if any movement is detected. This technique can be extended to two scanning orbits, one above and one below the sample plane to track the sample in 3D space. It can be used in vitro or in vivo to track a motion of a sample or to understand the dynamics of the sample. Additional detectors can help reveal the correlation between events with different emission spectrums. We have performed two different experiments with the system to show the capability of the technique. In the first example, we track a transcription site to understand the relationship between transcription factor - DNA binding and RNA transcription [1, 2]. By labeling a transcription factor with Halo-JF646 and nascent RNA with PP7-GFP, we were able to cross correlate fluorescence intensity to discover temporal coordination between transcription factor DNA binding and resulting gene activation. In the second experiment, we tracked lysosomes in live cells to understand the nature of the transport whether it is an active transport or a free diffusion [3]. Trajectories of a total of 24 lysosomes are recorded during the experiment. The mean squared displacement (MSD) curves of the trajectories showed some clear differences between the behaviors of the lysosomes which were attributed to the active transport along microtubules as opposed to freely diffusing lysosomes.

1. INTRODUCTION

In the last two decades many novel super-resolution microscopy techniques have been developed to image cellular structures beyond the diffraction limit. Some examples of these techniques are photo-activated localization microscopy (PALM) [4], stochastic optical reconstruction microscopy (STORM) [5-6], stimulated emission depletion (STED) [7] microscopy, near field scanning optical microscopy (NSOM) [8-9]. The significance of these developments led to a Nobel Prize in 2014 where Betzig, Moerner, and Hell were awarded the Nobel Prize for their contribution to development PALM (Betzig and Moerner) and STED microscopy (Hell).

Simultaneously, new techniques have been developed to study molecular dynamics of cellular structures[10-13]. Although the molecular dynamics of individual structures where initially deducted from the studies based on bulk

Single Molecule Spectroscopy and Superresolution Imaging XIII, edited by Ingo Gregor, Felix Koberling, Rainer Erdmann,
Proc. of SPIE Vol. 11246, 1124614 · © 2020 SPIE · CCC code: 1605-7422/20/$21 · doi: 10.1117/12.2546690

structures, recent technological improvements have provided new tools to understand the dynamics of an individual, single-molecule structure. Interests in biomolecular dynamics have been one of the major forces in developing super-resolution microscopy techniques, FLIM-FRET experiments, etc. Since structures drift or migrate over time, these techniques are time-limited when studying structures while they travel through the observation volume, which in turn affects the precision of the study. Many solutions have been proposed to extend experiment/observation periods. Some examples are attaching the biological structures to the surface to avoid or minimize drift or trapping the molecules in a capsule [14-17]. These methods are very perturbative processes since the results of experiments might strongly depend on the environment.

Independently, many methods were developed to track structures. Most of them use cameras as a part of wide-field imaging systems to track molecules [4-6, 18]. Post-process computer algorithms analyze data to build the trajectories that the structure took. These methods provide limited information on 3D trajectories. The 3D information is based on images recorded by microscopes with a modified optical path. One way to modify the optical path is by using a cylindrical lens in the optical path [19]. This results in astigmatism in the image which can be used to calculate the axial position of the structure. Another way is to obtain images from dual focal planes to determine the axial position of structures [19]. In either case, the range in which the structure can be determined is limited to a couple of micrometers of the imaging plane.

Another group of methods uses a closed-loop feedback system to control the scanning system of a confocal microscope [21-28]. These methods position the confocal volume of the excitation beam on the molecule of interest and collect its emission signal. The feedback system calculates the molecule's position as it drifts and in the millisecond temporal range the confocal volume is repositioned back on the molecule's position by the feedback system. These techniques have a wider spatial range of observation field of view, i.e. they can track an object for tens of micrometers in all directions including axial direction.

Here we discuss one of the methods that uses a closed-loop feedback system. It is called 3D orbital tracking. It was first proposed by Enderlein in 2000 [23] and was first implemented in 2003 by Gratton [24, 25]. It is based on a laser scanning confocal microscope. The Galvo mirrors of the microscope are driven to move the excitation beam in a circular orbit around a structure of interest such that the radius of the orbit is comparable to the radius of the confocal volume. The intensity of the fluorescence emission along the orbit is analyzed with a Fast Fourier Transform (FFT) based algorithm. The modulation of the first harmonic helps the feedback system calculate the size of the drift and the phase of the first harmonic helps it calculate the direction of the drift. Based on the calculations, the position information is used to update the center of the new circular orbit in the XY plane. The frequency of the orbits is limited by the Galvo mirror response time and is on the order of 1kHz. Generally, multiple orbits are scan before each feedback repositioning in order to reduce noise.

There are multiple ways to extend the technique to track particle in the axial direction [21, 23, 24, 29]. Our technique is extended to 3D by scanning two sets of orbits, one set of orbits scans above the structure and another one scans below the structure. A piezoelectric stage can be used to move the image plane relative to the sample to collect signals from two spatially separated orbits along the axial direction. The difference in the average intensity of the two orbits is used to localize the structure along the axial direction.

The response time of the piezoelectric stage is around 5ms and is the major limitation on this technique. Generally, the temporal resolution of this technique is around 32ms with a spatial resolution of 20nm in each direction. The structures with diffusivity up to 0.04 are successfully tracked with the 3D orbital tracking system.

This technique is very versatile as it can be implemented to various confocal microscopes even to a STED microscope [30]. In addition, data can be collected with multiple channels to study many biomolecular dynamics independently along the orbit.

Here we present two different applications as a proof of concept [1, 2, 3]. In the first experiment, a locus site of a cell is tracked and the characteristics of gene expression are studied over time in an Alba microscope. The main purpose of the experiment is to how the binding of a transcription factor correlates with transcriptional of RNA at an active gene. In the second experiment, lysosomes in live cells are studied with an Alba STED microscope. The

purpose of the experiment is to determine the type of transport whether it is an active transport or free diffusion of the lysosomes.

2. MATERIALS AND METHODS

2.1 The System Schematic

Figure 1 shows the schematic of a generic ISS Alba confocal microscope (http://www.iss.com/microscopy/instruments/albav5.html). Generally, Alba can host GaAsP (H7422p, by Hamamatsu), hybrid PMTs (R10467, by Hamamatsu), or avalanche photodiodes (APDs by Excelitas). Each excitation and emission dichroic wheels (D1 and D2) can hold 5 dichroic. Similarly, each filter wheel (EMs) can hold 5 filters. In an Alba, the detection channels are supported by dedicated variable pinhole apertures. The excitation chamber hosts Galvo mirrors (Cambridge Technologies). They are used to scan a raster image or an orbit in the XY image plane. The image plane is shifted by a high-speed piezoelectric stage (Nano-F25HS by MadCity Labs, Madison, Wi) during experiments in the axial axis. A long working distance objective is needed to avoid any crash between the objective and stage. Both of the experiments are performed on a Nikon Ti-U inverted microscope with a CFI Plan Apochromat 60X 1.2 NA water immersion objective (Nikon Instruments Incorporated, Melville, NY). The Galvo mirrors and the piezo device are controlled by an IOtech 3000 Data Acquisition card (Measurement Computing Corporation, Norton, MA). The same card is used to collect signals from the detectors. Data acquisition is performed by the SimFCS software (Laboratory for Fluorescence Dynamics, University of California, Irvine). Based on the feedback from the SimFCS, the IOTech card repositions the stage and centers the Galvo mirrors to compensate for the movement of the sample. The ISS Alba can be coupled to commercial microscopes from Olympus, Nikon or Zeiss.

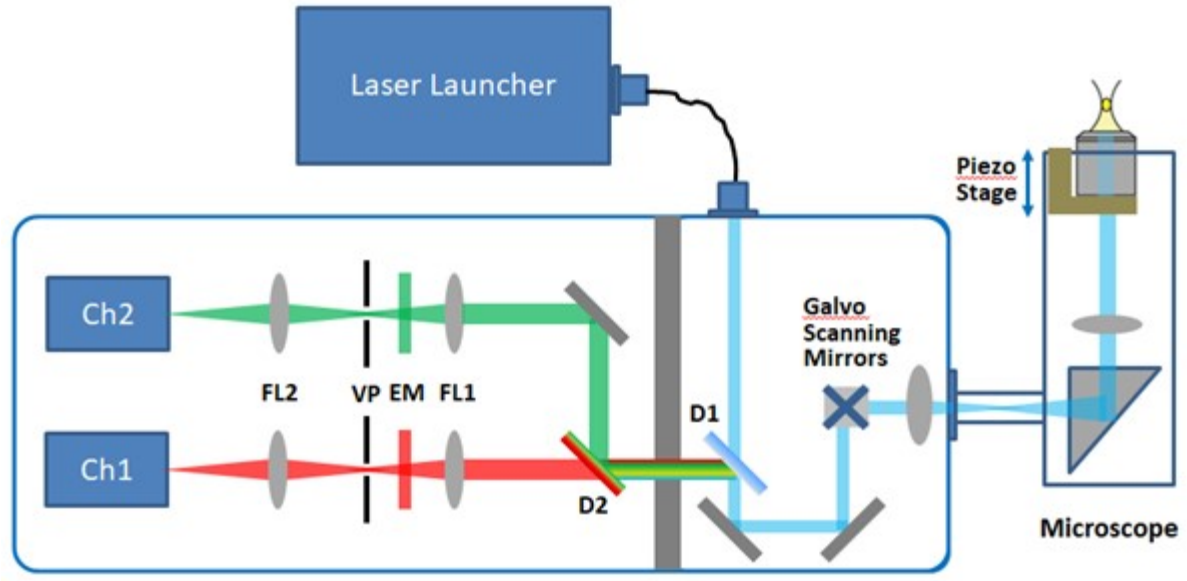

Figure 1. Schematic of Alba Confocal Microscope

For the gene expression experiments, the Alba confocal microscope was equipped with a 488nm laser and a 633nm laser. They were used in combination with a dual bandpass filter, zet488-640m (Chroma, Bellows Falls VT). The emission beam was split using a long-pass filter, et655lp (Chroma) and emission filters, ET700/75m (Chroma) and 525/50 (Semrock, Rochester NY). There were two SPCM-ARQH Avalanche Photodiode (Pacer, Palm Beach, FL)

detectors with dark counts <100/s. Alba was coupled to a Nikon Ti-U inverted microscope with a CFI Plan Apochromat 60X 1.2 NA water immersion objective (Nikon Instruments Incorporated, Melville, NY).

2.2 Tracking Procedure

An experiment starts by locating a particle of interest in a raster image in the XY plane. After setting up the tracking parameters like orbit radius, pixel-time, pixel numbers along an orbit, number of orbits, and the axial distance between two imaging planes, the center of the initial orbit is defined by clicking on the particle in the image. Once the tracking procedure starts, the excitation beam is driven on a circular orbit around the particle. In a typical experiment, 4 or 8 orbital periods are used for each feedback calculation. The half set of orbits is traced in the upper image plane and the other half is traced in the lower image plane. Figure 2a illustrates the upper and lower image plane orbits as well as a particle (black dot) and the point spread function of the excitation beam (blue oval volume). Figure 2b shows intensity profiles along the orbits. The blue curve shows the intensity profile during a feedback period from a simulation. In this example 4 orbits are scanned, two of them are in the first image plane and the other two are in the second image plane. As it is visible, the first two cycles have a higher intensity than the last two cycles have. This information is used to locate the axial position of the particle. The pink curve is the cumulative intensity profile for all the orbits. The shape of this profile is studied to extract location information of the particle on the XY image plane. The feedback algorithm analyzes the data on-fly to determine the coordinates of the particle and updates the scanner system to compensate for any particle movement.

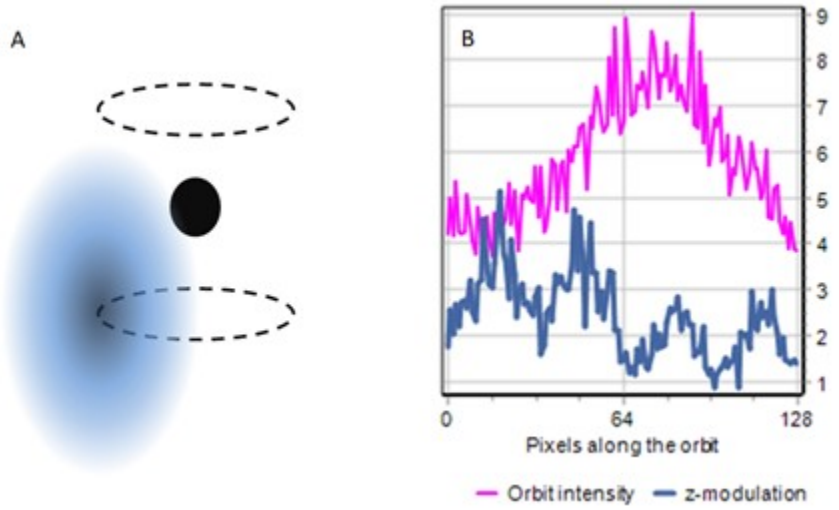

Figure 2: Schematic of a particle tracking experiment. (A) The panel shows the position of the point spread function of a laser beam relative to a particle. The upper and lower orbits are represented with dashed lines. (B) Intensity profiles along the orbit are shown here. The pink data is the cumulative intensity profile for all the orbits, and blue data shows the intensity profile for a feedback cycle. The system has scanned 4 orbits (2 up, 2 down orbits) for each feedback cycle in this example.

For the gene expression experiments, cells were labeled for 20 minutes with JF646 dye and grown or placed in 35mm dishes with #1.5 coverslips (Cellvis, Mountain View, CA). Cells were grown overnight in media and transcription was induced 10-20 minutes before imaging. Then they were placed inside a pre-warmed Okolab stage incubator maintained at a temperature of 37C, 5% CO2 (mammalian cells) and 100% humidity or 30C and 100% humidity (S. cerevisiae). The cells were kept in the incubator until transcription sites appeared. Transcription sites usually appeared as diffraction-limited spots inside the nucleus of a cell within 4 hours after induction. When an active transcription site was identified the laser power was lowered to reduce photobleaching and orbital tracking was initiated.

Tracking of transcription sites was tracked with four orbits with a ~87nm radius. The first two orbits were scanned 145nm above the transcription side followed by another two orbits 145nm below it. Each orbit consisted of 64 points

with a pixel dwell time of 1024 μs per pixel. Each orbit lasts 65.5ms with a total sampling time of 262 ms or a 3.8 Hz sampling rate for each feedback loop. The orbital tracking system tracked the fluorescently labeled transcription factor molecules in the red channel and saved the signal from RNA in the green channel simultaneously.

In the second experiment, lysosomes in live HeLa cells are tracked. The cells are incubated with LysoTracker Deep Red (ThermoFisher) at 75nM for two hours and then washed. An Alba-STED microscope is used to track the lysosomes. In this case, for the 3D, the microscope objective is mounted on a tunable lens (Optotune) instead of the piezo-electric stage. This allows much faster movement in the Z-direction since there is no actual motion of the objective, simply its focal length is electrically modified, at the cost of adding optics to the system and hence reducing the number of photons collected.

Lysosomes sites were tracked in multiple cells. Experiments lasted generally between 10 and 50 seconds. Orbital Tracking feedback algorithm parameters were chosen for best performance considering the relative brightness of the images and the observed speed of the lysosomes. Tracking was updated every four orbits for best signal to noise ratio. We used 64 points per orbit and a dwell time of 64μs per point, yielding an orbit time just over 4ms and of radius 70μm. An image was taken before and after each tracking experiment to check for instances of tracking jumping between lysosomes in cases of high density in the field of view.

3. RESULTS AND DISCUSSIONS

3.1 Gene Activation

When a sample is ready, it is imaged by repeated raster scans until the transcript site becomes active. Figure 3A and B shows two sample images where the transcript sites appeared as green dots in the RNA signal channel. Figure 3C shows an intensity profile along the orbit, the z and the intensity modulation. Figure 3D shows 3D-trajectory recorded during the experiment. Intensity profile along the orbit can be studied in "carpet plot"s during post data analysis. plot Figure 3E and 3F show examples of carpet plots. Carpet plots show fluorescence intensity along the orbit vs time. The pattern that is shown in the RNA channel (Figure 3E) confirms that the system tracked the particle without any suspicious activity like losing the site or jumping to another site. Simultaneously, the red channel records intensity signals from GR molecules. The carpet map of the red channel (Figure 3F) shows an intermittent signal in the red channel assumed to be binding of fluorescently labeled GR molecules.

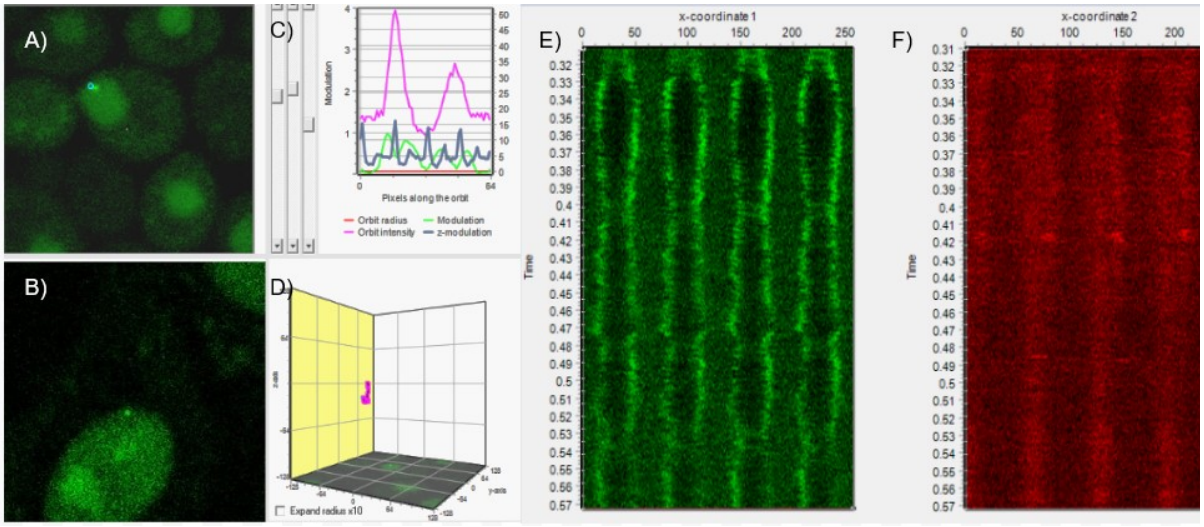

Figure 3: PP7 labeled transcription site screenshots in A) S. cerevisiae and B) Murine mammary epithelial cells. The nucleus of the cell is filled with GFP labeled PP7 coat protein. An active gene shows up as a diffraction-limited spot. C) Orbit intensity, modulation and z-modulation of orbital tracking. D) 3D trajectory of the transcription site during orbital tracking. E, F) Carpet plot of Green and Red signal during an orbital tracking experiment.

To test the correlation between the two channels, average intensity values along the orbit are calculated for both channels. Figure 4 shows such intensity profile over time for Gal10 RNA and Gal4 fluorescence emission. The initial rise in the intensity profile is usually due to lock-in on the transcription site. Sections of the fluorescence intensity traces which appear to be higher than the background level in the carpet plots were selected for active transcriptions. Auto and Cross correlation functions of the fluorescent signal were calculated in the standard way from the average fluorescence intensity traces. Early and late parts of the trace which included locking of the active feedback loop (~50 cycles) and initial strong photo-bleaching (~100 cycles) were excluded from analysis as were late parts of the traces of indefinite duration where the gene was no longer active (loss of green signal). Correlation functions were averaged over 10-20 measurements. In order to estimate the average number of molecules at the transcription site, the background fluorescence level was needed and was assumed to be equal to the minimum of fluorescence intensity traces over an entire measurement as described in [31]. This resulted in very robust and reproducible correlation functions from which the dwell time of transcription factor molecules, RNA and temporal relationships could be estimated as described above. Figure 4 insert shows an example of the correlation function which is obtained from the intensity profile data.

Correlation functions were fit to models using the LMFIT package [32] in python 2.7. For autocorrelation functions, a single component exponential or sinc function were used and for cross-correlation functions, a shifted Gaussian was used. Model fits were evaluated using Baysian Inference Criteria (BIC). The RNA autocorrelation was the best fit with a sinc function, transcription factor autocorrelation function was the best fit using a single exponential fit.
The cross-correlation of the two channels reveals the relationship between the activity on a Gal10 transcription site and the Gal4 binding process at the site. The intensity signals reveal that two events are correlated and the activity in the Gal4 channel lags the activity in the RNA Gal10 channel by 80 seconds.

Data analysis was performed using custom software written in IDL (Harris Geospatial Solutions, Broomfield CO) and Python 2.7 (Continuum Analytics, Austin, TX).

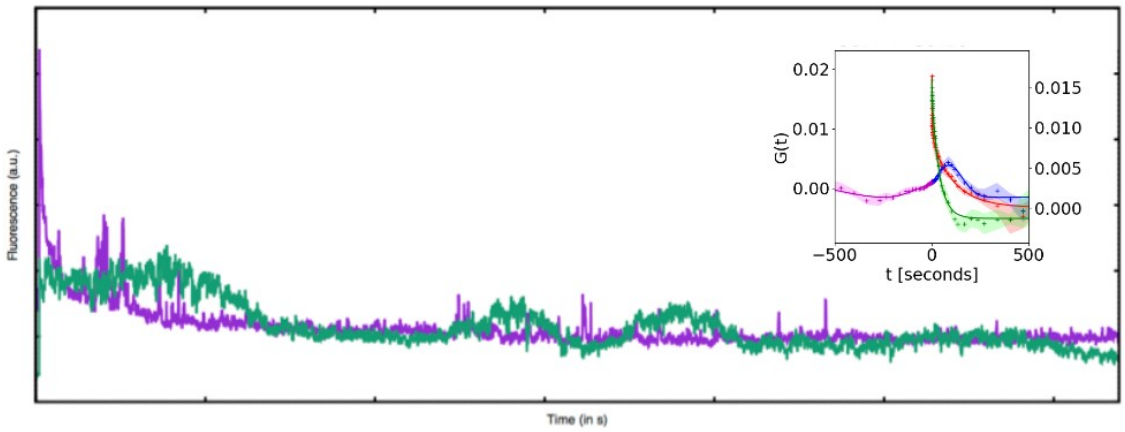

Figure 4: Characteristic trace of Gal4 and Gal10 RNA fluorescence intensity. (inset) Cumulative autocorrelation functions of Gal4 (red) and Gal10 RNA (green) as well as cross-correlation showing 60s delay between Gal4 binding and transcription of Gal10 RNA.

3.2 Transport of Lysosomes

A total of 24 lysosomes were tracked in different cells. Each experiment lasted between 10s and 50s. Experimental parameters were adjusted for the best performance considering the brightness and the speed of the particle, and the noise in the signal. Images of samples are recorded before and after the experiment to confirm the experimental success. Figure 5B shows a typical intensity vs feedback cycle graph. At the beginning of each experiment, there is usually a mismatch between the center of the first few cycles and the particle, which manifests as a lower intensity

value while the system locks on the particle, after which the intensity value rises once it is centered. As the experiment continues, the photo-bleaching results in decreasing intensity values. Figure 5A shows a trajectory of a lysosome in 3D. Based on trajectories, mean squared displacement (MSD) curves are calculated excluding the initial milliseconds where the intensity is still rising since it corresponds to the locking-on. Figure 5C and 5D show two distinct cases of MSD curves. In each curve, the brown area represents the variance of the MSD. The first part of the curves -initial 0.3s- is used to fit a straight line from which the 3D free diffusion MSD values are obtained (also called micro-diffusion). The cases in which the MSD curve tends to horizontal asymptote is attributed to confinements that limit the range a lysosome can travel in a free diffusion event, the cases in which the MSD curve increases with a trend above linearity is interpreted as case where the lysosome is attached to some molecular mechanism that is driving motion in a particular direction [3].

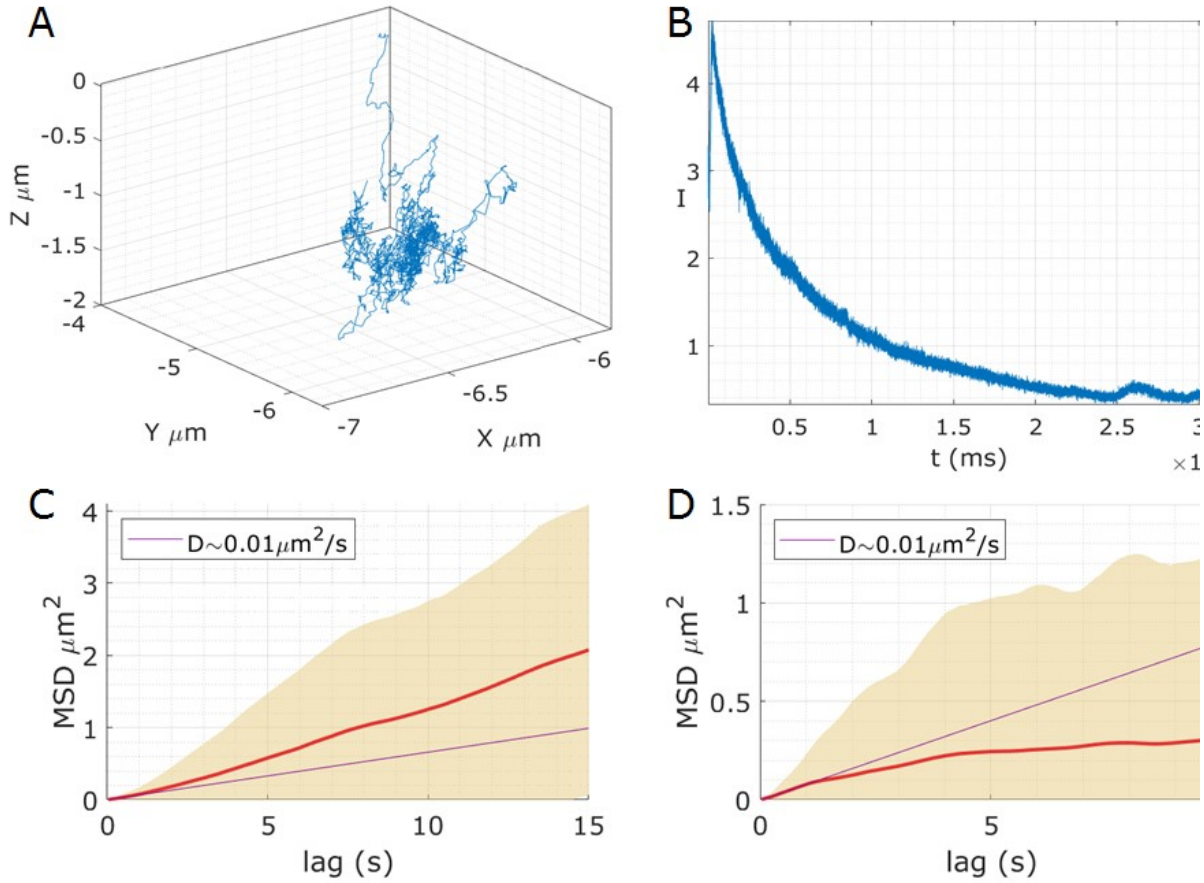

Figure 5: A) Example 3D trajectory of a lysosome. Initial drop in Z corresponds to the lock-in phase. B) Intensity profile during the tracking experiment. The decay in intensity is due to the photobleaching. C) MSD curve for a candidate of active transport. D) MSD curve for an example showing confinement.

Figure 6A shows all the MSD curves for all the 24 experiments together. Figure 6B summarizes all MSD values altogether in a single graph and Figure 6C presents the same data in a histogram. The average value for the MSD is calculated as 0.096 ± 0.004 μm²/s for 20 experiments after excluding 4 outlier values. This result is slightly above the reported value in the literature of 0.071μm²/s [33]. We consider the higher value as being due to the fact that the method we used to separate the outliers is somewhat arbitrary and/or an active transport process dominates the diffusion process.

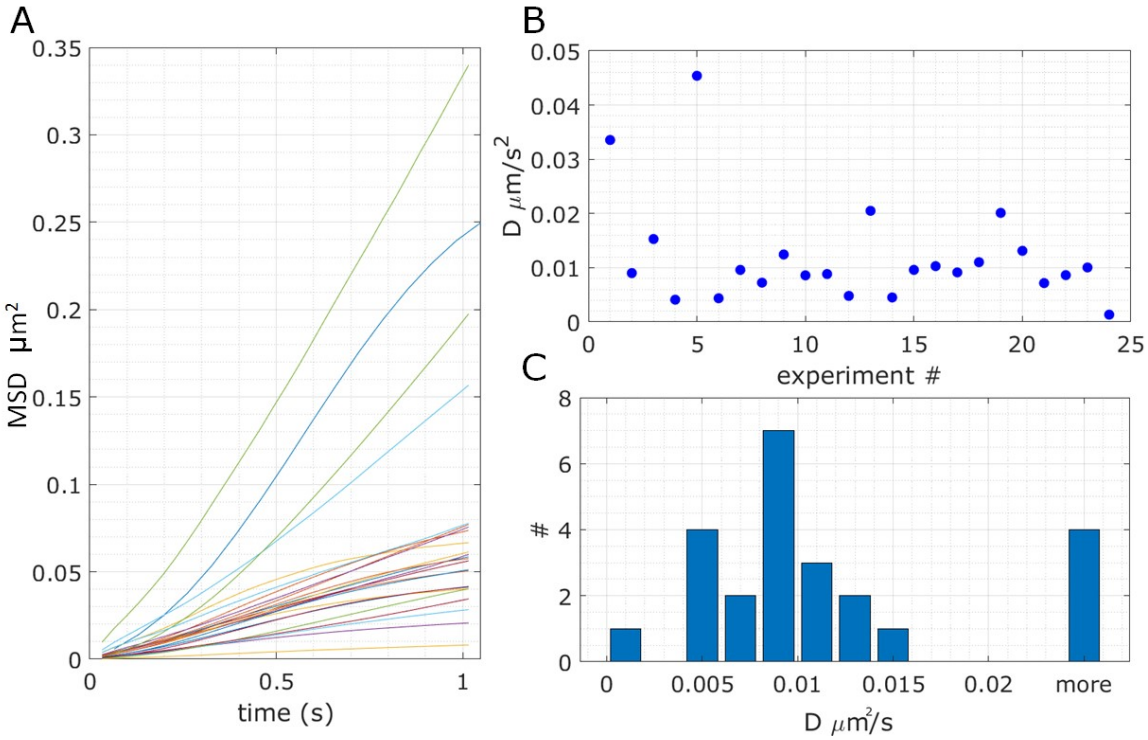

Figure 6: A) MSD curves for the 24 experiments. B) Micro-diffusion values obtained for each of them shown as a series. C) Histogram of the series with a binning of 0.002.

4. CONCLUSION

In conclusion, we integrated the 3D orbital tracking to an ISS Alba system. We have tested the system with two applications. In the first experiment, we track lysosomes with diffusion of 0.1µm²/s which would be very useful to study the motion of lysosomes and many other structures. In the second application, we have tracked an active transcription site. As we track the site, we have studied the activity of transcription in vivo which reveals a relationship, correlation, and timing between transcription factor bindings and transcription at the site. Briefly, the 3D particle tracking system provides a unique tool to track a site or molecule and study molecular dynamics in vivo as a function of the location.

ACKNOWLEDGMENTS

M.L.F., A.H. and J.G. were funded by Research Corporation for Science Advancement and the Gordon and Betty Moore Foundation through Grant GBMF5263.10 and by National Institute of General Medical Sciences through Grant 1R15GM123446-01. A.V. and E.G. were funded by NIH P41-GM103540.

REFERENCE

[1]. Stavreva, D.A., Garcia, D.A., Fettweis, G., Gudla, P.R., Zaki, G., Soni, V., McGowan, A., Williams, G., Huynh, A., Palangat, M., Schiltz, R.L., Johnson, T.A., Ferguson, M.L., Pegoraro, G, Upadhyaya, A., Hager, G.L., "Transcriptional bursting and co-bursting regulation by steroid hormone release pattern and transcription factor mobility." Molecular Cell. 2019.

[2]. Donovan, B.T., Huynh, A., Ball, D.A., Patel H.P., Poirier, M.G., Larson, D.L., Ferguson, M.L., and Lenstra, T.L.,"Live-cell Imaging Reveals the Interplay between Transcription Factors, Nucleosomes, and Bursting." The EMBO Journal 38, e100809 (2019).

[3]. Levi V, Gratton E., “Exploring dynamics in living cells by tracking single particles”. Cell Biochem Biophys. 48(1):1-15, (2007).

[4]. Betzig E, Patterson GH, Sougrat R, Lindwasser OW, Olenych S, Bonifacino JS, Davidson MW, Lippincott-Schwartz J, Hess H. “Imaging intracellular fluorescent proteins at nanometer resolution” Science 313(5793), 1642-5 (2006).

[5]. Rust MJ, Bates M, Zhuang X, “Sub-diffraction-limit imaging by stochastic optical reconstruction microscopy (STORM)” Nat Methods. 3(10), 793-5 (2006).

[6]. Zhuang X "Nano-imaging with Storm". Nature Photonics. 3 (7): 365–367, (2009).

[7]. Hell, S. W.; Wichmann, J. "Breaking the diffraction resolution limit by stimulated emission: Stimulated-emission-depletion fluorescence microscopy". Optics Letters. 19 (11), 780–782 (1994).

[8]. Synge, E.H. "A suggested method for extending the microscopic resolution into the ultramicroscopic region" Phil. Mag. 6, 356 (1928).

[9]. Synge, E.H."An application of piezoelectricity to microscopy", Phil. Mag., 13, 297 (1932).

[10]. Moerner, W.E., Orrit, M. “Illuminating Single Molecules in Condensed Matter”, Science, 283, 1670-1676 (1999).

[11]. Ha, T.; Enderle, T.; Ogletree, D.F.; Chemla, D.S.; Selvin, P.R.; Weiss, S. “Probing the interaction between two single molecules: Fluorescence resonance energy transfer between a single donor and a single acceptor”. Proc. Natl. Acad. Sci. 93, 6264 (1996).

[12]. Lu, H.P.; Xun, L.; Xie, X.S. “Single-Molecule Enzymatic Dynamics”. Science, 282, 1877–1882 (1998).

[13]. Shashkova, S.; Leake, M.C. “Single-molecule fluorescence microscopy review: Shedding new light on old problems”. Biosci. Rep., 37, BSR20170031 (2017).

[14]. Kudalkar, E.M.; Davis, T.N.; Asbury, C.L. “Single-Molecule Total Internal Reflection Fluorescence Microscopy”. Cold Spring Harbor Protocols 2016, pdb.top077800 (2016).

[15]. Leslie,S.R. Fields,A.P. Cohen,A.E. “Convex Lens Induced Confinement for Imaging Single Molecules”. Anal. Chem. 82, 6224–6229 (2010).

[16]. Kim, J.-Y.; Kim, C.; Lee, N.K. “Real-time submillisecond single-molecule FRET dynamics of freely diffusing molecules with liposome tethering”. Nat. Commun. 6, 6992 (2015).

[17]. Cohen, A.E., Moerner, W.E., “Controlling Brownian motion of single protein molecules and single fluorophores in aqueous buffer”. Opt. Express 16, 6941–6956 (2008).

[18]. Yildiz A., Forkey J.N., McKinney S.A., Ha T., Goldman Y.E., Selvin P.R, “ Myosin V walks hand-over-hand: single fluorophore imaging with 1.5-nm localization”. Science 300, 2061–5. (2003).

[19]. Kao, H.P., Verkman, A.S., “Tracking of Single Fluorescent Particles in 3 Dimensions - Use of Cylindrical Optics to Encode Particle Position”. Biophys. J. 67, 1291–1300 (1994).

[20]. Katayama, Y., Burkacky, O., Meyer, M., Brauchle, C., Gratton, E., Lamb, D.C. “Real-Time Nanomicroscopy via Three-Dimensional Single-Particle Tracking”. Chemphyschem 10, 2458–2464 (2009).

[21]. Berg, H.C. “How to Track Bacteria”. Rev. Sci. Instrum. 42, 868–871 (1971).

[22]. Lessard, G.A., Goodwin, P.M., Werner, J.H. “Three-dimensional tracking of individual quantum dots”. Appl. Phys. Lett.91, Artn 224106 (2007).

[23]. Cang, H., Wong, C.M., Xu, C.S., Rizvi, A.H., Yang, H., “Confocal three dimensional tracking of a single nanoparticle with concurrent spectroscopic readouts”. Appl. Phys. Lett. 88, Artn 223901 (2006).

[24]. Enderlein, J. “Tracking of fluorescent molecules diffusing within membranes”. Appl. Phys. B-Lasers O 71, 773–777 (2000).

[25]. Levi, V., Ruan, Q., Kis-Petikova, K., Gratton, E. “Scanning FCS, a novel method for three-dimensional particle tracking”. Biochem. Soc. Trans. 31, 997–1000 (2003).

[26]. Kis-Petikova, K., and Gratton, E. “Distance Measurement by Circular Scanning of the Excitation Beam in the Two-Photon Microscope.” Microscopy Research and Technique 63 (1) 34–49 (2004).

[27]. Germann, J.A., Davis, L.M., “Three-dimensional tracking of a single fluorescent nanoparticle using four-focus excitation in a confocal microscope”. Opt. Express 22, 5641–5650 (2014).

[28]. Hou, S.G., Lang, X.Q., Welsher, K. “Robust real-time 3D single-particle tracking using a dynamically moving laser spot”. Opt. Lett. 42, 2390–2393, (2017).

[29]. Annibale, P., Dvornikov, A,; Gratton, E. “Electrically tunable lens speeds up 3D orbital tracking”. Biomed. Optics Express 6, 2181–2190 (2015).

[30]. Vallmitjana-Lees A., Gratton E. “3D Orbital Tracking under STED Microscopy”. 63rd Annual Meeting of the Biophysical Society. Baltimore, MD. Biophysical Journal 116 (3), 440a, (2019).

[31]. Schwille, P., U. Haupts, S. Maiti, and W. W. Webb.“Molecular Dynamics in Living Cells Observed by Fluorescence Correlation Spectroscopy with One- and Two-Photon Excitation.” Biophysical Journal 77 (4): 2251–65 (1999).

[32]. Newville, M., T. Stensitzki, D. B. Allen, and A. Ingargiola.. “LMFIT: Non-Linear Least-Square Minimization and Curve-Fitting for Python” Doi: 10.5281/zenodo. 11813, (2014).

[33]. Bandyopadhyay D., Cyphersmith A., Zapata J. A., Kim Y. J., Payne C. K., "Lysosome Transport as a Function of Lysosome Diameter", Plos One, https://doi.org/10.1371/journal.pone.0086847 (2014)